Original Article

MOLECULAR METABOLISM

Altered function of arcuate leptin receptor expressing neuropeptide Y neurons depending on energy balance

Nicola J. Lee [1,2,3,*], Jennifer Oraha [1,2], Yue Qi [2], Ronaldo F. Enriquez [2], Ramon Tasan [4], Herbert Herzog [2,3]

ABSTRACT

Objective: One of leptin's main targets in the hypothalamus are neuropeptide Y (NPY) neurons, with selective deletion of leptin receptors (*Lepr*) specifically in *Npy* neurons resulting in major alterations of energy partitioning between fat and bone mass. However, the specific action of these *Npy*+/*Lepr*+ neurons compared to *Npy*-negative *Lepr* (*Npy*−/*Lepr*+) neurons in regard to energy homeostasis regulation is unknown.

Methods: Specific AAV viral vectors were generated using DREADD and INTRSECT technology and used in male $Lepr^{Cre/+}$ and $Lepr^{Cre/+}$; $Npy^{Flp/+}$ mice to assess the effect of activating either all *Lepr* neurons or specifically *Npy*+/*Lepr*+ or *Npy*−/*Lepr*+ neurons only on feeding, energy homeostasis control, and body composition.

Results: Selective stimulation of *Npy*+/*Lepr*+ neurons led to an immediate decrease in respiratory quotient followed by a delayed increase in food intake in standard chow fed, but interestingly not in high fat diet (HFD) fed mice. In addition, stimulation of *Npy*+/*Lepr*+ neurons led to a robust increase in brown adipose tissue thermogenesis and improved glucose tolerance. These effects were not observed in standard chow fed mice when *Npy*−/*Lepr*+ expressing neurons were specifically activated, suggesting the effects of leptin on these parameters are driven by NPY. However, under HFD condition when leptin levels are elevated, the stimulation of the *Npy*−/*Lepr*+ neurons increased food intake, physical activity and energy expenditure. Interestingly, chronic stimulation of *Npy*-positive *Lepr* neurons was able to increase bone mass independently of bodyweight, whilst chronic stimulation of the *Npy*−/*Lepr*+ neurons resulted in increased bodyweight and fat mass with proportionate increases in bone mass.

Conclusions: Together, these data indicate that leptin signalling through *Npy*-positive *Lepr*-expressing neurons controls energy partitioning via stimulation of thermogenesis, energy expenditure, and the use of fat as a fuel source. However, under prolonged HFD, leptin resistance may occur and actions of leptin signalling through *Npy*-negative *Lepr* hypothalamic neurons may exacerbate excess food intake.

Keywords NpyLeptin; DREADD; Food intake; Thermogenesis; Bone

1. INTRODUCTION

Leptin, an adipocyte-derived hormone primarily secreted in direct proportion to fat mass, is one of the main peripheral hormones that acts centrally on the hypothalamus to communicate energy status in the body. It acts in a negative feedback manner to inhibit anabolic (neuropeptide Y (NPY) neurons) and stimulate catabolic (proopiomelanocortin (POMC) neurons) effector pathways in the arcuate nucleus (Arc) of the hypothalamus thus supressing food intake and thereby preventing further weight gain [1]. In addition to its role in suppressing food intake, central leptin signalling has also been shown to impact energy expenditure, brown adipose tissue (BAT) thermogenesis, glucose and insulin homeostasis, as well as bone formation and resorption [2–5]. However, there is still much that remains unknown in terms of the specific neuronal populations and circuits mediating these various effects.

Recent studies have highlighted the functional diversification that exists within classically defined neuronal populations such as NPY and POMC neurons. Two largely non-overlapping subpopulations of POMC neurons have been described defined on either leptin receptor (*Lepr*) or glucagon like receptor 1 (*Glp1r*) expression with each subpopulation displaying distinct electrophysiological properties, anatomical distribution, and ability to suppress feeding [6]. It is likely that such complexity also exists with respect to the effects of leptin on NPY neurons. Indeed, Baskin et al. [7] have shown that in fed rats, only 47% of *Npy* neurons in the Arc also express the *Lepr*. Furthermore, whilst Arc *Npy* neurons have classically been defined as co-expressing *Agrp*, recent data from our group and others show that approximately 20% of Arc *Npy* neurons do not express *Agrp* [8,9]. Importantly, we have shown that *Lepr* expression is higher in the subpopulation of *Npy* neurons that do not co-express *Agrp* [10], supporting the idea that specific sub-populations of NPY neurons exist that specialise in

[1]Charles Perkins Centre, School of Medical Sciences, Faculty of Medicine and Health, University of Sydney, NSW, Australia [2]Garvan Institute of Medical Research, NSW, Australia [3]St Vincent's Clinical School, UNSW Sydney, NSW, Australia [4]Institute of Pharmacology, University of Innsbruck, Austria

*Corresponding author. Charles Perkins Centre, The University of Sydney, NSW 2006, Sydney, Australia. E-mail: nikki.lee@sydney.edu.au (N.J. Lee).

Received June 25, 2023 • Revision received July 31, 2023 • Accepted August 5, 2023 • Available online 9 August 2023

https://doi.org/10.1016/j.molmet.2023.101790

controlling specific physiological functions. This is further supported by the fact that whilst no impact of *Lepr* deletion in *Agrp* neurons was found on bone mass [11], the deletion of *Lepr* from *Npy* neurons led to significantly increased adiposity and diminished bone mass [10]. These body composition changes occurred in the absence of alterations in food intake or energy expenditure, demonstrating a prominent role for leptin signalling through NPY neurons in the control of energy partitioning. Interestingly, when fed a high fat diet (HFD), these mice displayed a switch in energy partitioning whereby they exhibited a significantly enhanced ability to increase their bone mass to match the increased body weight caused by higher caloric intake concurrent with attenuated adiposity [10].

In order to characterise the specific *in vivo* actions that *Npy*-positive (*Npy*+) versus *Npy*-negative (*Npy*−) hypothalamic neurons play in leptin's control of energy homeostasis, we have employed intersectional Cre/Flp-dependent chemogenetically modifiable designer G-protein-coupled receptors (hM3Dq) delivered via AAV viral methodology into $Lepr^{Cre/+};Npy^{Flp/+}$ mice. This approach allowed us to specifically investigate the functional role of *Npy*+/*Lepr*+ neurons compared to that of *Npy*−/*Lepr*+ neurons in the metabolic regulation of energy homeostasis and body composition.

2. MATERIALS AND METHODS

2.1. Animals

$LepR^{cre/+}$ (B6.129(Cg)-$Lepr^{tm2(cre)Rck}$/J) mice (JAX #008320) were crossed with $Npy^{flp/+}$ (B6.Cg-$Npy^{tm1.1(flop)Hze}$/J) mice (JAX #030211) to generate $Lepr^{Cre/+};Npy^{Flp/+}$ mice. Genotyping was performed by PCR using genomic DNA isolated from tail tips. All animal experiments used male mice and were approved by the Garvan Institute/St Vincent's Hospital Animal Experimentation Ethics Committee and conducted in accordance with relevant guidelines and regulations. Mice were housed under conditions of controlled temperature (22 °C ± 1 °C) with a 12-h light, 12-h dark cycle (lights on at 0700). Mice had *ad libitum* access to either a standard chow diet (8% calories from fat, 21% calories from protein, 71% calories from carbohydrate, and 3.1 kcal/g; Gordon's Speciality Stock Feeds, Yanderra, NSW, Australia) or a high-fat diet (HFD; 43% calories from fat, 17% calories from protein, 40% calories from carbohydrate, and 4.78 kcal/g; Specialty Feeds, Glen Forrest, WA, Australia) from 8 weeks of age. Body weight was monitored weekly.

2.2. AAV vectors

AAV vectors containing Cre-inducible versions of the stimulatory hM3D(Gq) or inhibitory hM4Di DREADD receptors as well as an AAV-GFP control vector were used as previously published [12]. An AAV vector containing the stimulatory hM3Dq DREADD construct fused to a YFP cassette in the $Cre_{on};Flp_{off}$ configuration was used as previously published and allows for the production of a functional transcribable DREADD-YFP unit only when Cre-recombinase is present, but prevents it if flipase is present on its own or in combination with Cre-recombinase [9]. A second AAV vector containing the stimulatory hM3Dq DREADD construct fused to an *mCherry* cassette but in the $Cre_{on};Flp_{on}$ configuration was generated based on the same strategy [13]. For this vector, the specific combination of *loxP* and *Flp* sites in a 'flip and excise' (FLEX) orientation, combined with the introduction of introns in specific locations allows for rearrangements of the transcription unit that results in the production of a functional transcribable DREADD-mCherry unit only when both Cre-recombinase and flipase are present, but prevents it if either are present on their own. Details of the design of both the $Cre_{on};Flp_{off}$ and the $Cre_{on};Flp_{on}$ vectors is shown in Supplementary Figure 1.

2.3. Brain injections for adeno associated virus (AAV)-DREADD

Ten-week-old mice were fully anaesthetised with saline-diluted ketamine/xylazine cocktail according to their bodyweight and placed on the stereotaxic frame. Surgical incisions were made through full anatomic layers of the skin and periosteum along the midline to expose the skull. A microinjection needle was adjusted over the brain towards the arcuate nucleus (Arc; −1.8 mm from Bregma and 0.25—0.3 mm off the midline) according to the coordinates from The Mouse Brain in Stereotaxic Coordinates [14]. A hole was then drilled through the skull and dura mater and saggital sinus followed by the inserton of the injection needle. The depth of the injection was also adjusted to speficially target the Arc (5.7 mm from the surface of the brain); 0.75 μL of the injection solution containing AAV (4×10^{12}) was then slowly injected over 5 min, and the needle was left in place for another 10 min to prevent reflux. The same procedure was performed on the contralateral side. After the injection and removal of the needle, the wound was sutured and the animal was housed individually in a cage with a heating pack until it fully woke up. Medical indications including bodyweight, physical movement and infection were regularly monitored for two weeks after the injection until the mice were fully recovered. Accuracy of injections were confirmed by fluorescent microscopy after cull as described below. DREADD receptors were stimulated with intraperitoneal injections of clozapine-N-oxide (CNO) at a dose of 10 mg per kg bodyweight. CNO treatments were randomly alternated with control treatments of 10 μL per g bodyweight saline unless stated.

2.4. Metabolic phenotyping of mice

Indirect calorimetry measurements on mice were performed using the Promethion metabolic cage system (Sable Systems International, Las Vegas, NV, USA). Mice were single housed and acclimatised in the Promethion cages for 72 h before data acquisition. The Promethion multiplexed system has a home-like environment with each cage containing standard bedding, a food hopper, a water bottle, and an enrichment tube for body mass measurements, all connected to load cells for real-time weight monitoring. Instrument control and data acquisition were performed according to the manufacturer's instructions. Raw data was processed using ExpeData software (Sable Systems).

Glucose tolerance tests (GTT) were performed twice, one week apart beginning at 14 weeks of age with randomly alternating intraperitoneal injections of CNO or saline given at 2 pm 30 min prior to the intraperitoneal glucose bolus (1.0 g/kg) following a 5 h fast. Blood glucose levels were measured in tail blood using an Accu-Check ® Go glucometer (Roche, Dee Why, NSW, Australia) immediately before both CNO/saline and glucose injections and again at 15, 30, 60 and 90 min post glucose injection.

2.5. Thermal imaging

To study body and brown adipose tissue temperatures, non-invasive high-sensitivity infrared imaging was performed. 72 hr prior to data acquisition, animals were single housed and allowed to acclimatise to the experimental room under standard housing conditions. 24 hr prior to imaging, mice had approximately 2 cm^2 of their interscapular and lumbar back skin shaved, under light isoflurane anaesthesia in order to expose the skin of these areas for accurate temperature readings. On the day of imaging, a high-sensitivity infrared camera (ThermoCAM

T640, FLIR, Danderyd, Sweden, sensitivity = 0.04 °C, IR resolution = 640 × 480 pixels) fixed on a tripod was placed 90 cm above the freely moving mice to record the surface temperatures of the mice in a 30–60 s video (image frequency = 30 Hz) at baseline. Immediately following basal recordings, animals were injected intraperitoneally with either CNO or saline and videos were again acquired at 15, 30, 45, 60, 120, and 180 min following CNO/saline treatment. Animals remaining single housed until the procedure was repeated the following day with randomly alternating CNO/saline injections. Where thermal imaging was performed under cold stress conditions, the cages and camera were placed in a 4 °C chamber immediately following basal recordings and CNO/saline injections. Following the 180 min recording, mice were returned to room temperature and videos were again acquired at 240 and 360 min following CNO/saline treatment. Thermo-frames (5 per timepoint per mouse) that had the mice walking or standing still with their body naturally extended and both shaved skin regions vertical to camera lenses were extracted from the videos for analysis. Extracted images were analysed using the FLIR ResearchIR MAX 4.40 software to obtain body and brown adipose tissue temperatures.

2.6. Body composition

The effect of short-term chronic stimulation of DREADD receptors on body composition was performed in mice at 16–17 weeks of age. Mice were randomly allocated to either a CNO or saline control group. On the Friday, 3 days prior to treatment beginning, body composition including lean mass, fat mass, bone mineral content (BMC) and bone mineral density (BMD) were measured in mice anaesthetised with isoflurane using an UltraFocus Faxitron (Faxitron Bioptics, LLC, Tucson Az, USA). At this time, mice were injected intraperitoneally with 15 mg/kg of the fluorescent tetracycline compound calcein (Sigma). CNO/saline treatments were given daily for 5 consecutive days (Monday–Friday) with the 4th dose combined with a second dose of calcein. One week after the initial assessment and coinciding with the final CNO/saline treatment dose, body composition was re-measured using the Faxitron. Mice were culled the following Monday, 3 days later.

2.7. Tissue collection

At 17 weeks of age, mice were culled by perfusion 1 h following randomly allocated intraperitoneal CNO or saline. Briefly, after complete anaesthesia, mice were perfused with 0.9% saline through the left ventricle, followed by 4% paraformaldehyde perfusion until the whole body was fully fixed. The brain was removed from the skull, placed in fixative over 24 h at 4 °C, and kept in 30% glucose in PBS over 24 h or until the brain sunk at 4 °C and then stored at −80 °C until further use. Femurs were excised, fixed overnight in 4% paraformaldehyde (PFA) in phosphate buffered saline (PBS) at 4 °C and then stored in 70% ethanol at 4 °C before undergoing processing.

2.8. Isolated bone measurements

Cortical mineral apposition rate was measured in an endosteal region using fluorescent microscopy and 5 μm sagittal sections of the distal half of the right femur as previously described [15].

2.9. Fluorescent immunohistochemistry

Fixed brains were cryo-sectioned at 40 μm thickness and stored in cryoprotectant at 4 °C prior to immunohistochemical staining. Brain sections were incubated in citrate buffer (0.1 M Citric Acid, 0.1 M Trisodium citrate) in a water bath for 5 min at 65 °C. Following incubation in the citrate buffer, sections were washed four times in 1× PBS for 5 min. The sections were then incubated in 10% normal goat serum for 1 h to block non-specific binding sites, followed by incubation in 1× PBS containing 5% goat serum, 0.2% triton X100, 0.1% bovine serum albumin, and affinity purified antibodies at 4 °C overnight with gentle shaking. Primary antibodies used were rabbit anti-cFOS (1:500; Sigma-Aldrich), anti-GFP (1:1000, Invitrogen) and anti-mCherry (1:1000, Abcam) or, when used in combination with the anti-Flp antibody, chicken anti-GFP (1:1000, Abcam) and anti-mCherry (1:1000, Abcam). Sections were then washed four times in 1× PBS for 5 min and incubated with secondary antibodies in 1× PBS containing 5% goat serum, 0.2% triton X100, 0.1% bovine serum albumin for 1 h at room temperature with gentle shaking. Secondary antibodies used were donkey anti-rabbit Cy3 antibody (1:500; Jackson ImmunoResearch Laboratories, Inc), donkey anti-sheep Alexa 488 antibody (1:500, Thermofisher), and goat anti-chicken IgY 488 and 555 antibodies (both 1:500, Abcam). Sections were then washed four times in 1× PBS for 5 min, mounted onto slides and cover-slipped with antifading mount media (Fluoroshield with DAPI, Sigma-Aldrich). Sections were examined and imaged using either a Leica DM 5500 fluorescent microscope and attached camera (DFC310Fx) or a Nikon C2 Confocal Microscope.

To quantify cFOS expression between groups, 5 brains per group were processed for immunohistochemistry with the anti-cFOS primary antibody. One in every four rostral to caudal sections throughout the Arc were selected for each brain and the number of cFOS positive neurons in the Arc was quantified using ImageJ software.

2.10. Statistical analyses

All data are expressed as means ± SEM. Differences between groups were assessed using student's *t* test, ANOVA followed by Bonferroni's multiple comparisons post hoc test, or repeated measures ANOVA where appropriate. Statistical analyses were performed with Prism, version 9 (GraphPad Software Inc, La Jolla, CA, USA). $p < 0.05$ was taken to be statistically significant.

3. RESULTS

To determine the actions that *Npy*-positive versus *Npy*-negative neurons play in leptin signalling, we used a viral DREADD approach combined with INTRSECT methodology [13]. Specifically, we targeted *Npy*+/*Lepr*+ neurons in the Arc using an AAV viral vector expressing the stimulatory hM3D(Gq) DREADD receptor in a Cre-on/Flp-on specific manner in $Lepr^{Cre/+};Npy^{Flp/+}$ mice (Figure 1A and Supplementary Figure 1A). A second vector was used to express the same DREADD receptor in a Cre-on/Flp-off manner [9] (Figure 1B and Supplementary Figure 1B), thus targeting the *Lepr*-positive neurons which do not express *Npy* (*Npy*−/*Lepr*+ neurons). The entire Arc *Lepr*-positive neuronal population were also either stimulated or inhibited in $Lepr^{Cre/+}$ mice with previously published Cre-induced versions of the hM3D(Gq) or hM4Di, respectively [12]. Mice injected with an AAV-GFP virus were used as additional controls. Correct injection sites and anatomical expression were confirmed by immunohistochemistry evaluation of mCherry/EYFP as appropriate. As shown in Figure 1C, the Cre-on/Flp-on version of the vector specifically targeted a subpopulation of *Npy*-expressing neurons in the Arc with little expression seen elsewhere. Co-localisation of mCherry with Flp expression by IHC confirms that this vector successfully targeted *Npy* neurons (Figure 1F). In contrast, the Cre-on/Flp-off vector successfully targeted non-*Npy* expressing neurons in the Arc as shown by the lack of co-localisation between GFP and Flp in Figure 1G, but also spread to other regions including the dorsomedial hypothalamic nucleus (DMH), the lateral hypothalamus (LHA), and the ventral premammillary nucleus

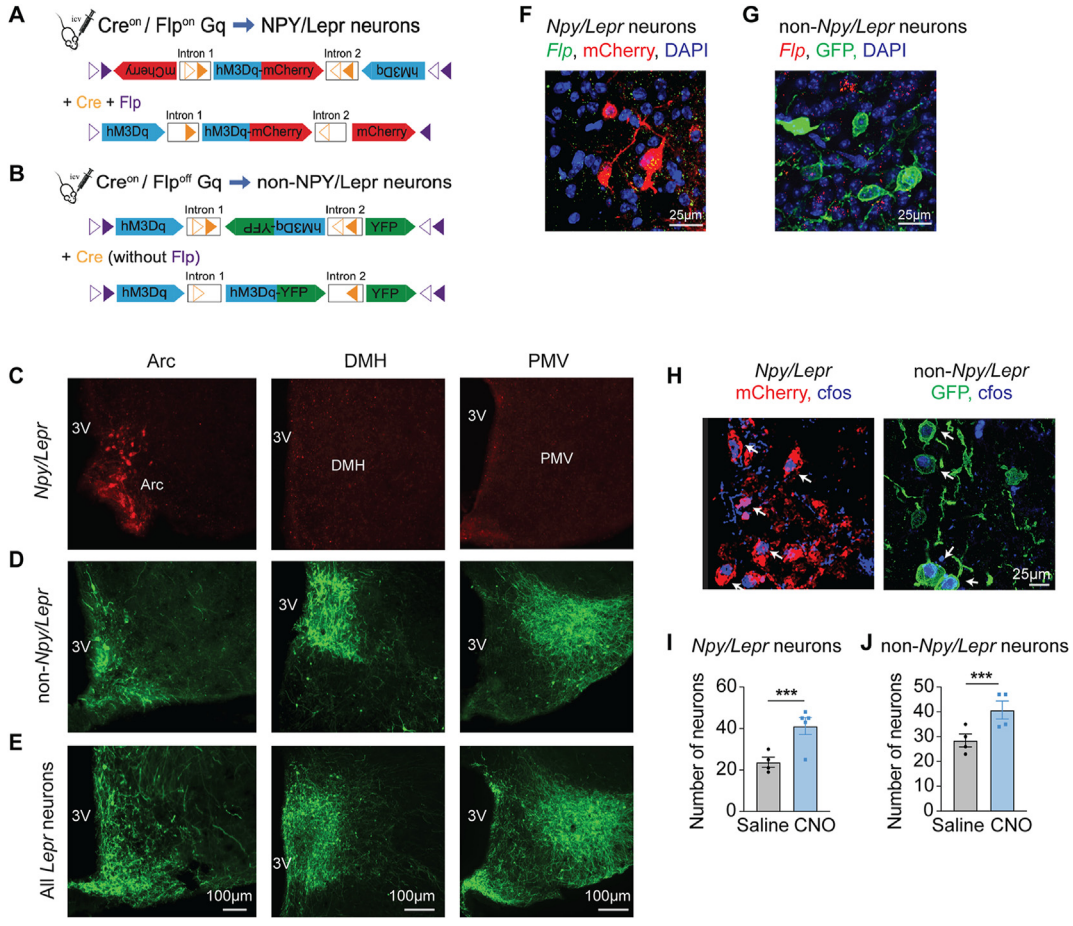

Figure 1: AAV vector expression and validation. Schematic diagrams showing (A) the Cre_{on};Flp_{on} AAV vector and (B) the Cre_{on};Flp_{off} AAV vector both containing the stimulatory DREADD hM3Dq fused with either (A) an mCherry reporter or (B) a YFP reporter used to selectively activate (A) *Npy*+/*Lepr*+ neurons and (B) *Npy*−/*Lepr*+ neurons. Representative fluorescent images showing successful expression of (C) the Cre_{on};Flp_{on} AAV vector in $Lepr^{Cre/+}$, $Npy^{Flp/+}$ mice targeting *Npy*+/*Lepr*+ neurons (red), (D) the Cre_{on};Flp_{off} AAV vector in $Lepr^{Cre/+}$, $Npy^{Flp/+}$ mice targeting *Npy*−/*Lepr*+ neurons (green), and (E) a Cre induced AAV vector also containing the hM3Dq DREADD in $Lepr^{Cre/+}$ mice targeting all *Lepr* neurons (green). Representative fluorescent images showing (F) co-localisation of the mCherry reporter (red) from the Cre_{on};Flp_{on} AAV vector with Flp (green) expressed under control of the *Npy* promotor by immunohistochemistry and (G) lack of co-localisation of the YFP reporter (green) from the Cre_{on};Flp_{off} AAV vector with Flp (red) expressed under control of the *Npy* promotor by immunohistochemistry. (H) Representative fluorescent images and (I–J) quantification of CNO induced cFos expression (blue) in $Lepr^{Cre/+}$, $Npy^{Flp/+}$ mice injected with both the Cre_{on};Flp_{on} AAV vector targeting *Npy/Lepr* neurons (red) and the Cre_{on};Flp_{off} AAV vector targeting non-*Npy/Lepr* neurons (green). Data are means ± SEM of at least 4 per group. Data analysed by Student's t-test. *** = $p < 0.001$ as indicated.

(PMV) (Figure 1D). The Cre-induced version of the hM3D(Gq) vector targeted all *Lepr* neurons with expression seen in the Arc as well as in similar areas (DMH, LHA and PMV) to that shown by the Cre-on/Flp-off vector (Figure 1E). Functionality of the Cre-on/Flp-on and Cre-on/Flp-off pAAV vectors was confirmed by immunohistochemistry showing that CNO induced Fos expression in mCherry/EYFP positive neurons (Figure 1H, quantified in I–J).

3.1. *Npy*+/*Lepr*+ neurons control fuel choice with a delayed effect on food intake

To determine the contribution of different populations of *Lepr*-positive neurons in the Arc in the control of feeding and energy homeostasis, comprehensive metabolic profiling was performed on DREADD injected mice receiving randomly alternating CNO or saline treatments so that they can act as their own controls and the effect on metabolic parameters was monitored for the subsequent 6-h period where CNO exerts its main effect (Figure 2A). Importantly, CNO treatment in AAV-GFP injected control mice did not have any significant effect on any of the parameters investigated under either fed or fasted conditions (Supplementary Figure 2). Next, we investigated the effect of stimulating all *Lepr*-positive Arc neurons using an AAV-hSyn-DIO-hM3D(Gq)-mCherry vector injected bilaterally into the Arc of $Lepr^{Cre/+}$ mice. To also evaluate the influence of differing activity states of the mice, CNO treatment in these mice was performed either at 9 am during the light phase, when mice normally eat and move less, as well as at 4 pm just before the onset of the dark phase when mice increase their activity and feeding behaviour. Interestingly, when stimulated at 9 am, activation of these neurons did not result in any significant effect on food intake (Figure 2B). However, a significant increase in energy expenditure was observed without any change in physical activity but accompanied by a significant decrease in respiratory quotient (RQ) (Figure 2C–E, time course shown in Supplementary Figure 4). In contrast, these changes in energy expenditure and RQ were not observed when treatment was given at 4 pm prior to the onset of the dark phase (Figure 2C–E) or when treatment was given at 9 am concurrent with the re-introduction of food following a 24 h fast

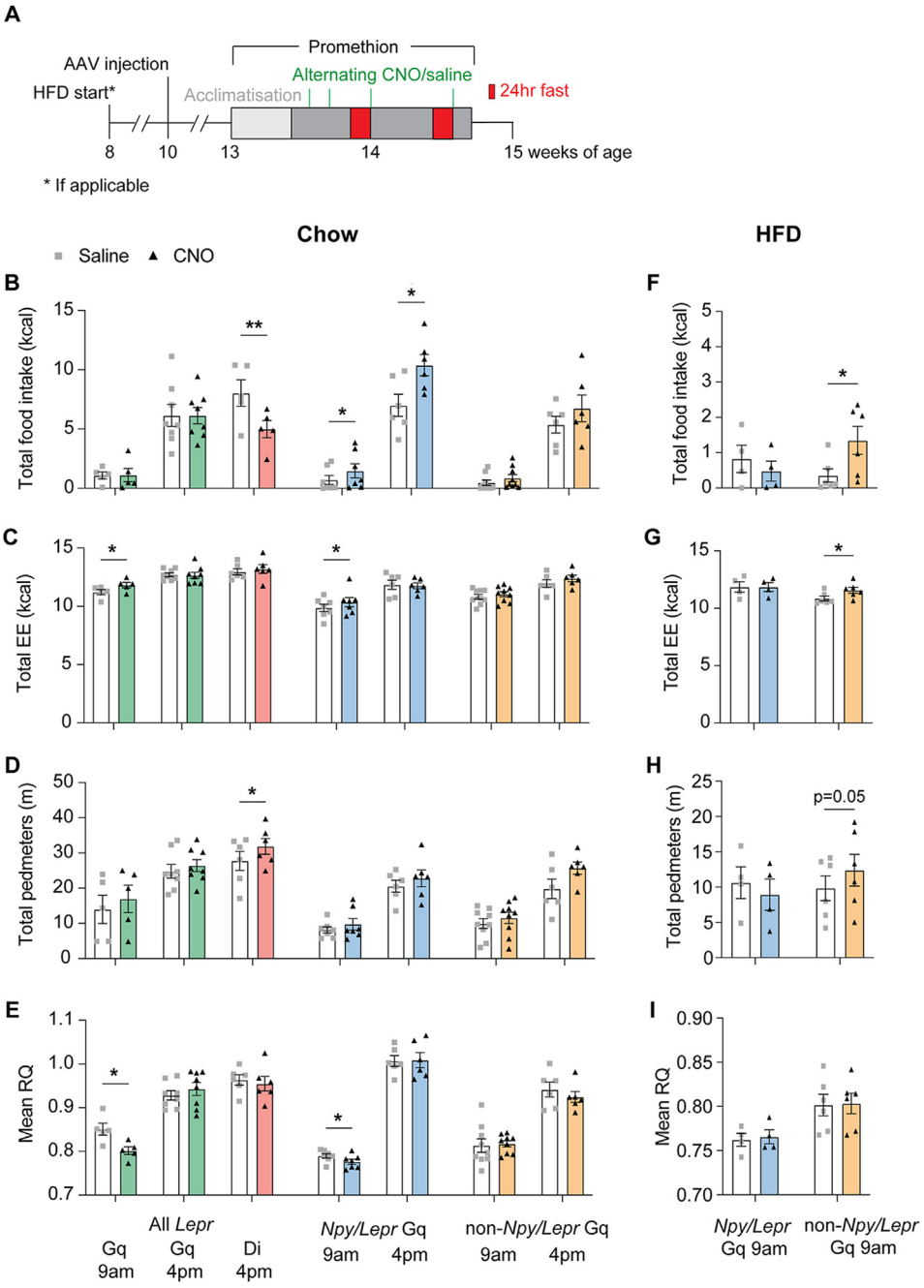

Figure 2: *Npy*+/*Lepr*+ neurons control fuel choice with a delayed effect on food intake whilst *Npy*−/*Lepr*+ neurons drive food intake under high fat diet fed conditions. (A) Promethion schedule. (B) Food intake (FI), (C) energy expenditure (EE), (D), distance in voluntary locomotion (pedmeters) travelled, and (E) mean respiratory quotient (RQ) for the 6 h time period following CNO or saline treatment in chow-fed mice when either all *Lepr* neurons are stimulated (Gq) or inhibited (Di), or specifically *Npy*+/*Lepr*+ or *Npy*−/*Lepr*+ neurons are stimulated. CNO/saline treatment was given at either 9 am or 4 pm as indicated. (F) Food intake (FI), (G) energy expenditure (EE), (H), distance in voluntary locomotion (pedmeters) travelled, and (I) mean respiratory quotient (RQ) for the 6 h time period following CNO or saline treatment at 9 am in high fat diet (HFD)-fed mice when either specifically *Npy*+/*Lepr*+ or *Npy*−/*Lepr*+ neurons are stimulated. Data are means ± SEM of at least 5 per group. Data analysed by paired Student's t-tests. NS = not significant, * = $p < 0.05$, ** = $p < 0.01$ as indicated.

(Supplementary Figure 3A–D). On the other hand, the inhibition of all Arc *Lepr*-expressing neurons using a pAAV-hSyn-FLEX-hM4Di-mCherry virus injected bilaterally into the Arc of *Lepr*$^{Cre/+}$ mice and CNO treatment starting at 4 pm in *ad libitum* fed animals led to a significant decrease in total food intake (Figure 2B). Surprisingly, despite CNO treatment also resulting in increased physical activity levels (Figure 2D), the reduced food intake did not lead to altered energy expenditure or RQ values (Figure 2C, E and time course shown in Supplementary Figure 4). Again, these effects were not evident when treatment was given concurrent with the re-introduction of food following a 24 h fast (data not shown), although we did observe that CNO treatment led to a delay in the start of food consumption following the re-introduction of food compared to when they were treated with saline (Time to first removal of food from hopper: saline:

62.5 ± 19.14 min; CNO: 160.0 ± 19.2 min; p = 0.003), suggesting some inhibition of the drive to eat.

In order to investigate the specific effect of leptin signalling through *Npy*+/*Lepr*+ neurons, metabolic profiling was performed in $Lepr^{Cre/+}$;$Npy^{Flp/+}$ mice injected bilaterally in the Arc with an AAV-nEF-Con/Fon-hM3D(Gq)-mCherry virus. Again, CNO/saline treatment was given at both 9 am during the light phase and 4 pm just prior to the onset of the dark phase. Stimulation of *Npy*+/*Lepr*+ neurons with CNO led to an increase in food intake, which was more pronounced when CNO was given at 4 pm (Figure 2B). Interestingly however, this was a delayed effect with the increase only beginning 4 h after CNO treatment (Supplementary Figure 4C). Whilst stimulation of *Npy*+/*Lepr*+ neurons at 9 am led to a significant increase in energy expenditure throughout the 6-h time period following CNO treatment, this was not evident at the 4 pm treatment time and no effect on physical activity was observed during either treatment period (Figure 2C–D). Interestingly, a significant drop in RQ in the first 3 h following treatment was observed which was more pronounced at the 9 am treatment time despite no change in activity or food intake during this period (Figure 2E and Supplementary Figure 4). No significant effects of *Npy*+/*Lepr*+ neuronal stimulation were observed in any parameters when treatment was given at 9 am concurrent with food being returned following a 24 h fast suggesting that fasting-induced pathways override any leptin signalling via NPY neurons (Supplementary Figure 3A–D).

In contrast, the specific stimulation of *Npy*−/*Lepr*+ neurons using an AAV-hSyn-Con/Foff-hM3D(Gq)-EYFP virus injected bilaterally into the Arc of $Lepr^{Cre/+}$;$Npy^{Flp/+}$ mice and subsequent CNO treatment at either 9 am or 4 pm did not result in any significant treatment effects on food intake, energy expenditure, physical activity, or RQ (Figure 2B–E and time course shown in Supplementary Figure 4). Again, no differences were observed when treatment was given at 9 am as food was returned following a 24 h fast (Supplementary Figure 3A–D).

3.2. *Npy*−/*Lepr*+ neurons drive food intake under high fat diet fed conditions

Despite leptin's anorectic effects, obesity is characterised by elevated leptin levels and the development of leptin resistance [16]. Several mechanisms have been identified as potentially underlying the development of leptin resistance including defects in the transport of leptin across the blood brain barrier and altered downstream intracellular signalling mechanisms [17,18]. To investigate whether leptin signalling in the Arc is altered under situations of chronically elevated leptin and obesity, we stimulated *Npy*+/*Lepr*+ and *Npy*−/*Lepr*+ neurons in the Arc with CNO in DREADD injected $Lepr^{Cre/+}$;$Npy^{Flp/+}$ mice which had been fed a HFD for 6 weeks. As the effect of stimulating *Npy*+/*Lepr*+ neurons in chow-fed mice were more pronounced at the 9 am treatment time, we used this protocol for the HFD-fed experiments. Importantly, CNO treatment in AAV-GFP injected control mice that had also been fed a HFD diet did not have any significant effect on any of the parameters investigated under either fed or fasted/re-fed conditions (Supplementary Figure 2). Interestingly, the effects seen upon stimulation of *Npy*+/*Lepr*+ neurons under standard chow conditions were not evident under HFD conditions with no significant treatment effects observed in food intake, energy expenditure, physical activity or RQ in either the fed state (Figure 2F–I) or when treatment was given concurrent with re-feeding after a 24 h fast (Supplementary Figure 3E–H). Furthermore, and again in contrast to chow fed mice, the stimulation of *Npy*−/*Lepr*+ neurons led to a significant increase in total food intake associated with a significant increase in energy expenditure and a trend towards increased physical activity, but no change in RQ (Figure 2F–I). Most of these effects, apart from increased physical activity, were over-ridden by fasting induced re-feeding (Supplementary Figure 3E–H). Together these data suggest that *Lepr*-expressing *Npy* neurons may become resistant to the effects of chronically elevated leptin levels under obese conditions whilst *Npy*−/*Lepr*+ neurons may drive excess food intake under HFD-fed conditions.

3.3. *Npy*+/*Lepr*+ neurons increase brown adipose tissue thermogenesis

Neuronal activation of *Lepr* expressing neurons in the DMH/DHA with DREADDs has been shown to increase both brown adipose tissue (BAT) and body temperature [19]. Therefore, we used thermal imaging combined with randomly alternating injections of CNO or saline (Figure 3A) to investigate whether *Lepr* expressing neurons in the Arc also play a role in thermal regulation, and whether this involves *Npy* signalling. No significant effects on either BAT or back temperature were observed with CNO treatment in AAV-GFP injected controls (Supplementary Figure 5A–C). Interestingly, although no significant differences in either BAT or back temperature were observed when either all Arc *Lepr* expressing neurons or *Npy*−/*Lepr*+ neurons were stimulated under standard room temperature conditions (Supplementary Figure 5D–I), a significant increase in BAT but not back temperature was observed in response to CNO stimulation of *Npy*+/*Lepr*+ neurons in the Arc (Figure 3B–E). Consistent with previous results, the ability of *Npy*+/*Lepr*+ neuronal stimulation to increase BAT thermogenesis was no longer evident in mice fed a HFD for 4 weeks (Figure 3F–H). No differences in either BAT or back temperature were observed when *Npy*−/*Lepr*+ neurons were stimulated under HFD fed conditions (Supplementary Figure 5J–L).

To also determine whether these neurons play a role during cold stress, we repeated the thermal imaging experiments placing the mice in a 4 °C chamber following initial baseline readings and CNO/saline injections. Again, no significant effects were observed in either BAT or back temperature or the difference between them when AAV-GFP injected controls were treated with CNO (Supplementary Figure 5M–P) or when *Npy*−/*Lepr*+ neurons were stimulated (Supplementary Figure 5Q–T). However, CNO stimulation of *Npy*+/*Lepr*+ neurons led to an increase in BAT temperature as well as a decrease in back temperature during cold exposure resulting in a significantly greater difference in BAT versus back temperature compared to saline treatment (Figure 3I–L). These data suggest a specific role for leptin via NPY neurons in regulating thermogenesis under both normal and cold stress situations.

3.4. *Npy*+/*Lepr*+ neurons act to improve glucose tolerance under high fat diet conditions

Leptin has been shown to have beneficial effects on glucose and insulin homeostasis by decreasing glycaemia, insulinemia and insulin resistance through both central, hypothalamic mediated effects as well as peripheral effects in the pancreas, muscle and liver [20]. To investigate the specific role of NPY versus non-NPY neurons in leptin's regulation of glucose tolerance, we performed intraperitoneal glucose tolerance tests on DREADD injected mice beginning 30 min after CNO/saline administration. Glucose tolerance tests were performed twice on each mouse, one week apart, with randomly allocated CNO or saline so that they could act as their own controls. No significant effect of CNO treatment was observed on glucose or insulin levels throughout the glucose tolerance test in AAV-GFP injected control mice (Figure 4A–D). No differences were also observed in glucose or insulin levels throughout the glucose tolerance test when either *Npy*−/*Lepr*+

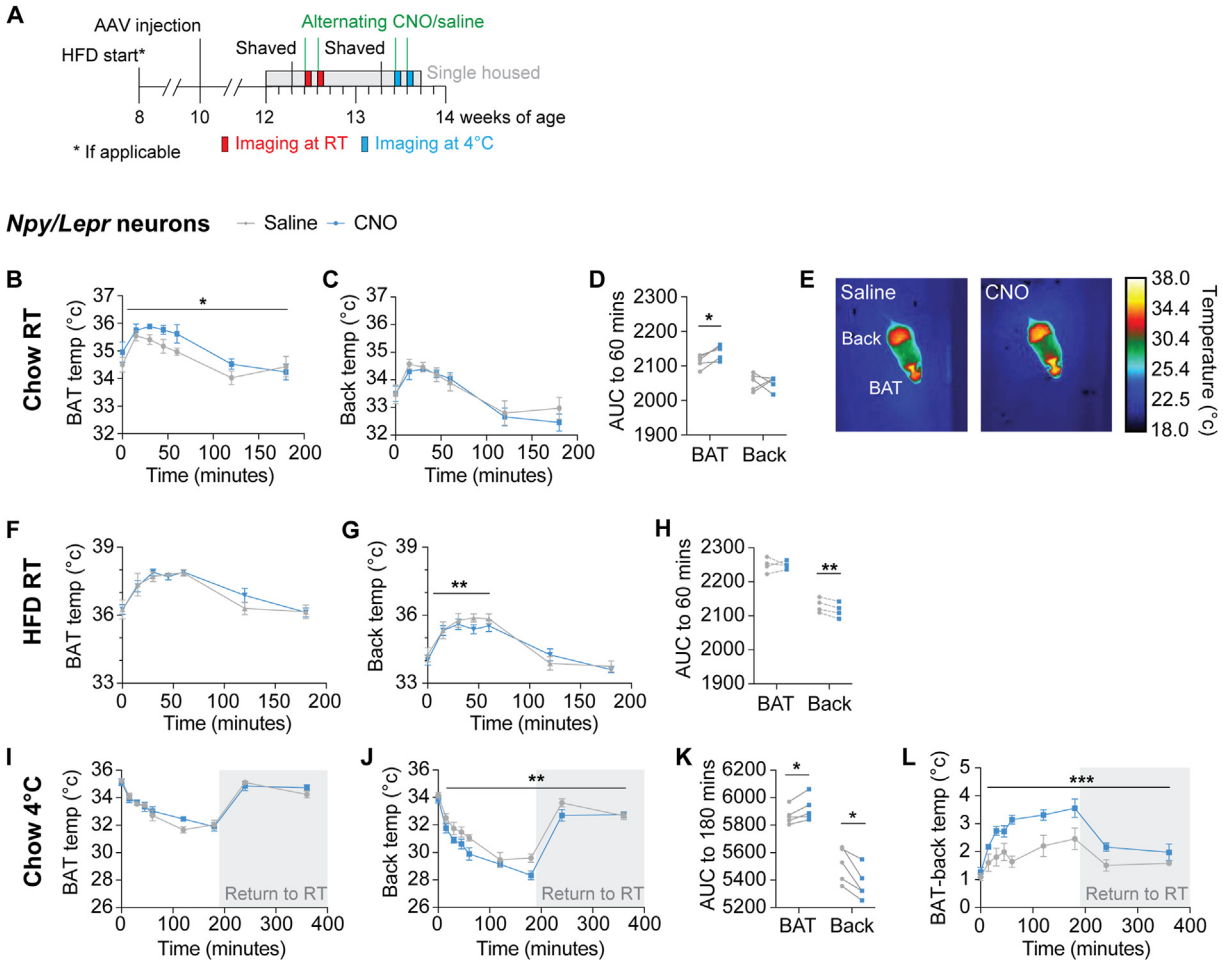

Figure 3: *Npy+/Lepr+* neurons increase brown adipose tissue thermogenesis. (A) Thermal imaging schedule. (B) Brown adipose tissue (BAT) temperature and (C) back temperature over time, (D) area under the curve (AUC) for BAT and back temperature from 0 to 60 min, and (E) representative images showing BAT and back temperature at 30 min timepoint following CNO/saline treatment in chow-fed $Lepr^{Cre/+}$, $Npy^{Flp/+}$ mice injected with a stimulatory hM3D(Gq) DREADD virus targeting *Npy+/Lepr+* neurons. (F) BAT temperature and (G) back temperature over time, and (H) AUC for BAT and back temperature from 0 to 60 min following CNO/saline treatment in high fat diet (HFD)-fed $Lepr^{Cre/+}$, $Npy^{Flp/+}$ mice injected with a stimulatory hM3D(Gq) DREADD virus targeting *Npy+/Lepr+* neurons. (I) BAT temperature and (J) back temperature over time, (K) AUC for BAT and back temperature from 0 to 180 min following CNO/saline treatment, and (L) difference between BAT and back temperature over time in chow-fed $Lepr^{Cre/+}$, $Npy^{Flp/+}$ mice injected with a stimulatory hM3D(Gq) DREADD virus targeting *Npy+/Lepr+* neurons under cold stress conditions. Shaded grey area represents time when mice are returned to room temperature conditions. Data are means ± SEM of at least 5 per group. Data analysed by repeated measures two-way ANOVA with Bonferonni's multiple comparisons post-hoc test except for AUC comparisons which were analysed by paired Student's t-tests. * = $p < 0.05$, ** = $p < 0.01$, *** = $p < 0.001$ as indicated.

neurons or *Npy+/Lepr+* neurons were stimulated with CNO under chow fed conditions (Figure 4E—H). However, when mice had been fed a HFD for 8 weeks, *Npy+/Lepr+* stimulation led to improved glucose levels throughout the glucose tolerance test due to elevated insulin secretion (Figure 4I—L). As a result, whilst saline treated and *Npy—/Lepr+* stimulated mice on HFD showed the expected hyperglycaemia, *Npy+/Lepr+* stimulated mice had similar glucose area under the curve values to chow-fed mice (Figure 4M). These data suggest that leptin signalling through NPY neurons is able to regulate insulin secretion and glucose tolerance even under conditions of elevated leptin levels.

3.5. Differing effects of *Npy+/Lepr+* versus *Npy—/Lepr+* neurons on body composition

We have previously shown a role for leptin signalling through NPY neurons in the control of energy partitioning, with chow-fed mice lacking *Lepr* on *Npy* neurons displaying increased adiposity concurrent with reduced bone mass [10]. To further investigate this and also determine whether non-NPY neurons play a role in leptin's control of energy partitioning, we used chronic daily stimulation over 5 days of *Npy+/Lepr+* and *Npy—/Lepr+* neurons and investigated the effect on body composition (Figure 5A). Whilst AAV-GFP injected control mice treated with CNO did display a significant decrease in fat mass and an increase in lean mass over the treatment period, these changes were not significant when analysed as weight change within individual mice and no changes in body weight or bone parameters were observed (Supplementary Figure 6A—J). A similar effect was seen when another group of DREADD injected $Lepr^{Cre/+}$;$Npy^{Flp/+}$ mice were treated with saline (Figure 5B—K) and thus is likely a result of either age or the repetitive injections, not CNO itself. No additional significant effects were seen when all *Lepr* expressing neurons in the Arc were chronically stimulated with CNO compared to saline treated mice (Supplementary Figure 6M—V). However, specific chronic stimulation of *Npy—/Lepr+* neurons led to an increase in bodyweight over the

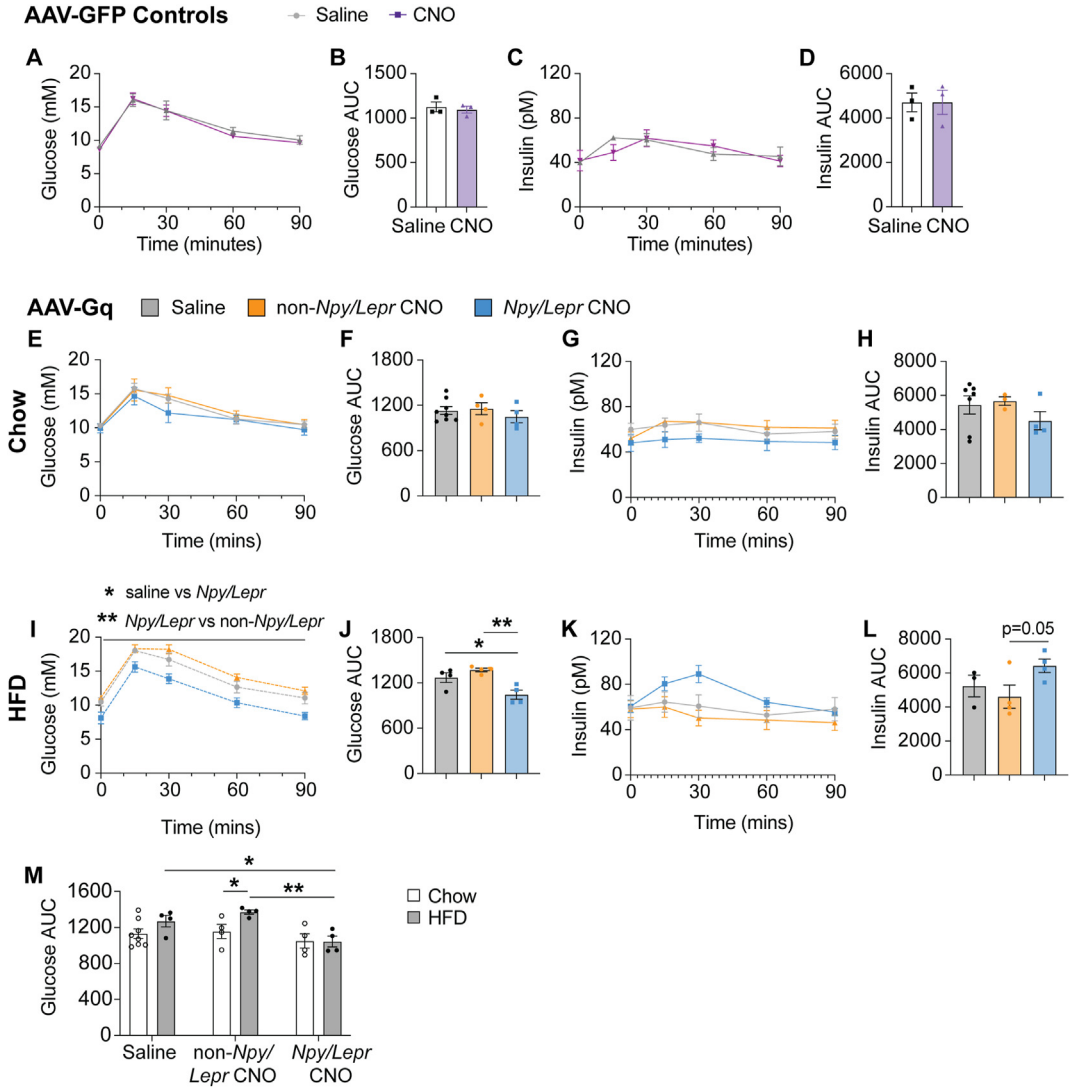

Figure 4: *Npy+/Lepr+* neurons act to improve glucose tolerance under high fat diet conditions. (A—B) Glucose and (C—D) insulin levels during a glucose tolerance test shown either as (A, C) a time course or (B, D) expressed as area under the curve (AUC) for chow-fed $Lepr^{Cre/+}$ mice injected with an AAV-GFP control virus and treated with either CNO or saline. (E—F, I—J, M) Glucose and (G—H, K—L) insulin levels during a glucose tolerance test shown either as (E, G, I, K) a time course or (F, H, J, L, M) expressed as AUC for (E—H) chow-fed or (I—L) high fat diet (HFD)-fed $Lepr^{Cre/+}$, $Npy^{Flp/+}$ mice injected with a stimulatory hM3D(Gq) DREADD virus targeting either *Npy+/Lepr+* neurons or *Npy—/Lepr+* neurons and treated with either CNO or saline. (M) Comparison of glucose levels between chow-fed and HFD-fed mice. Data are means ± SEM of at least 4 per group. Data analysed by (A, C, E, G, I, K) repeated measures two-way ANOVA with Bonferonni's multiple comparisons post-hoc test, (B, D) Student's t-test, (F, H, J, L) one-way ANOVA or (M) two-way ANOVA with Bonferonni's multiple comparisons post-hoc test. * = $p < 0.05$, ** = $p < 0.01$ as indicated.

treatment period which was not evident in saline treated mice (Figure 5B) and they did not display the reduction in fat mass and increase in lean mass seen in saline treated mice (Figure 5C—D). Indeed, when analysed as weight change within individual mice, *Npy—/Lepr+* stimulated mice showed a significant increase in bodyweight as well as fat mass but no change in lean mass compared to saline treated mice (Figure 5G—I). Consistent with the increased bodyweight, *Npy—/Lepr+* stimulated mice also showed a significant increase in whole body bone mineral content (BMC) but not bone mineral density (BMD) over the treatment period compared to saline treated mice (Figure 5E—F, J—K). Of note, there was no change in the correlation between bodyweight and BMC in these *Npy—/Lepr+* neuron stimulated mice suggesting that the increase in BMC was proportionate to the increase in bodyweight (Figure 5M). However, although CNO stimulation of *Npy+/Lepr+* neurons did not alter bodyweight, fat mass, or lean mass (Figure 5B—D, G—I), we did observe a trend towards an increase in BMC over the treatment period compared to saline treated mice (Figure 5E, J). This led to a disassociation in the correlation between bodyweight and BMC suggesting that the stimulation of *Npy+/Lepr+* neurons may be able to alter bone mass independent of bodyweight (Figure 5N).

3.6. Leptin affects bone formation through both *Npy* and non-*Npy* neurons

Consistent with the whole body faxitron data, no change in isolated femoral BMC or BMD was observed following cull in either AAV-GFP injected control mice treated with CNO or following chronic CNO stimulation of all *Lepr* neurons (Supplementary Figure 6K—L, W—X). However, isolated femoral BMC was significantly higher in the *Npy—/Lepr+* neuron chronically stimulated mice compared to saline but not

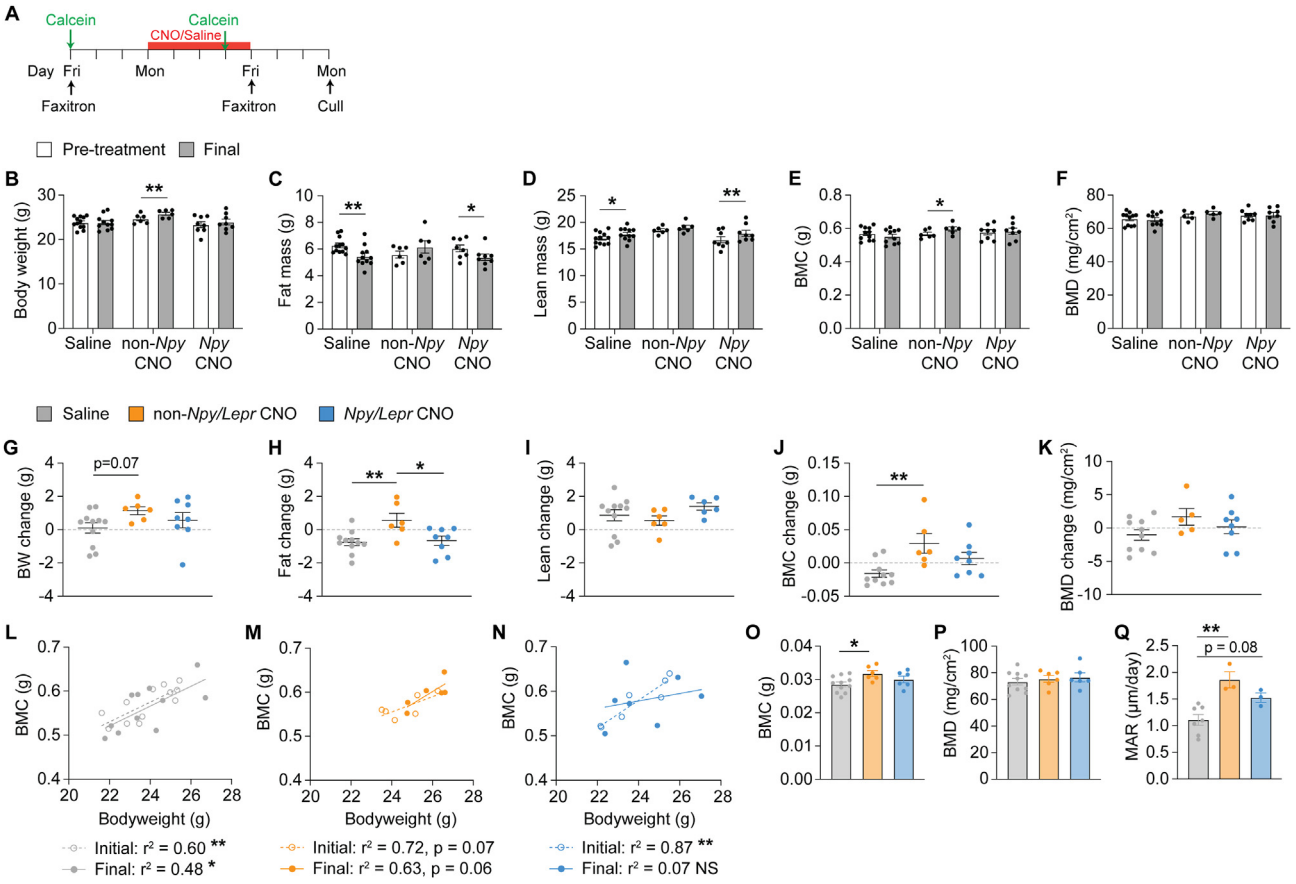

Figure 5: Differing effects of *Npy*+/*Lepr*+ versus *Npy*−/*Lepr*+ neurons on body composition. (A) Chronic CNO/saline treatment schedule. (B) Body weight, (C) fat mass, (D) lean mass, (E) bone mineral content (BMC), and (F) bone mineral density (BMD) before and after chronic CNO/saline treatment in $Lepr^{Cre/+}$, $Npy^{Flp/+}$ mice injected with a stimulatory hM3D(Gq) DREADD virus targeting either *Npy*−/*Lepr*+ neurons (On/Off virus) or *Npy*+/*Lepr*+ neurons (On/On virus). Change in (G) body weight, (H) fat mass, (I) lean mass, (J) BMC, and (K) BMD following chronic CNO/saline treatment in $Lepr^{Cre/+}$, $Npy^{Flp/+}$ mice injected with a stimulatory hM3D(Gq) DREADD virus targeting either *Npy*−/*Lepr*+ neurons (On/Off virus) or *Npy*+/*Lepr*+ neurons (On/On virus). (L–N) Correlation between body weight and BMC following chronic CNO/saline treatment in $Lepr^{Cre/+}$, $Npy^{Flp/+}$ mice injected with a stimulatory hM3D(Gq) DREADD virus targeting either *Npy*−/*Lepr*+ neurons (On/Off virus) or *Npy*+/*Lepr*+ neurons (On/On virus). (O) BMC, (P) BMD, and (Q) cortical mineral apposition rate (MAR) in femora isolated after cull from $Lepr^{Cre/+}$, $Npy^{Flp/+}$ mice injected with a stimulatory hM3D(Gq) DREADD virus targeting either *Npy*−/*Lepr*+ neurons or *Npy*+/*Lepr*+ neurons and chronically treated with CNO or saline. Data are means ± SEM of at least 6 per group. Data analysed by (B–F) repeated measures two-way ANOVA with Bonferonni's multiple comparisons post-hoc test, (G–K, O–Q) one-way ANOVA, or (L–N) linear regression. NS = not significant, * = $p < 0.05$, ** = $p < 0.01$ as indicated.

in the *Npy*+/*Lepr*+ neuron stimulated mice (Figure 5O–P), consistent with the changes in bodyweight and BMC observed from the whole-body scans. In order to determine whether the change in BMC was caused by alterations in bone formation, a subset of the mice was injected with calcein twice spanning the treatment period, enabling the measurement of mineral apposition rate (MAR) (Figure 5A). Consistent with the increased BMC observed in both *Npy*+/*Lepr*+ and *Npy*−/*Lepr*+ stimulated mice, MAR was increased in both groups, albeit this did not reach statistical significance in the *Npy*+/*Lepr*+ stimulated group (Figure 5Q).

4. DISCUSSION

By using novel, sophisticated viral vectors expressing stimulatory DREADD receptors in a Cre and Flp dependent manner in our $Lepr^{Cre/+}$;$Npy^{Flp/+}$ mice, we have dissected the specific metabolic role of NPY neurons versus non-NPY neurons in mediating leptin's effects in the Arc. The widely accepted model is that leptin acts as a satiety signal by inhibiting anabolic NPY/AgRP neurons and stimulating catabolic POMC/CART neurons. However, the heterogeneity now evident within these neuronal populations combined with the myriad of effects that leptin has on metabolism and body composition, suggests that greater complexity exists in leptin's interaction with hypothalamic neurons than the model suggests. Here, we show that stimulating only those *Npy* neurons that express the *Lepr* leads to decreased RQ, a delayed increase in food intake, increased BAT thermogenesis, improved glucose tolerance, and increased bone mass independent of body-weight. Importantly, we show that the ability of *Npy*+/*Lepr*+ neurons to regulate RQ, food intake, and BAT thermogenesis is compromised under conditions of elevated leptin levels induced by HFD feeding. In contrast, *Npy*−/*Lepr*+ neurons appear to be hypersensitive after HFD and may be involved in exacerbating food intake under obese conditions.

We have previously shown that *Lepr* expression is higher in the portion of *Npy* neurons that do not express *Agrp* [10]. Importantly, here we show that specifically stimulating the *Npy*+/*Lepr*+ neurons results in effects different to those seen when *Agrp*-negative *Npy* neurons were stimulated using the same DREADD methodology, identifying a distinct role for *Npy*+/*Lepr*+ neurons and highlighting the complexity that exists within the Arc *Npy* neuronal population. The stimulation of

Agrp-negative *Npy* neurons led to increased food intake but, in contrast to *Npy*+/*Lepr*+ stimulation, this effect was more pronounced in response to both HFD feeding and re-feeding following a fast [9]. Also, in contrast to *Npy*+/*Lepr*+ stimulation, no differences in energy expenditure or RQ were observed when *Agrp*-negative *Npy* neurons were stimulated under normal chow conditions although these parameters were both increased with HFD feeding [9].

One of the predominant effects of central leptin signalling is to inhibit food intake, thereby preventing further weight gain. In this study, the effects of stimulating *Lepr* expressing neurons on food intake were mild. Nevertheless, the inhibition of all hypothalamic *Lepr* neurons using the inhibitory DREADD in $Lepr^{Cre/+}$ mice did result in a significant reduction in food intake, whilst stimulating them did not result in increased food intake. This suggests that under normal conditions the hypothalamic effect of leptin on food intake is primarily driven by the neurons it inhibits (anabolic NPY/AgRP neurons). Consistent with this, we saw an increase in food intake with the specific stimulation of *Npy*+/*Lepr*+ neurons in our $Lepr^{Cre/+}$;$Npy^{Flp/+}$ mice but no effect when *Npy*−/*Lepr*+ neurons were stimulated confirming a predominant role for NPY neurons in this process. This effect was no longer evident in HFD-fed mice suggesting that the signalling potential of these neurons is substantially altered under conditions of elevated leptin levels.

Aside from food intake, the metabolic effects of leptin include an increase in energy expenditure, increased lipolysis (decrease RQ), increased BAT thermogenesis, and decreased glucose levels. Therefore, the fact that stimulating *Npy*+/*Lepr*+ neurons led to decreased RQ, increased BAT thermogenesis, and improved glucose tolerance is somewhat contrary to that expected from the stimulation of neurons that leptin has been shown to inhibit. Nevertheless, these parameters were unaltered by the stimulation of *Npy*−/*Lepr*+ neurons, clearly implicating NPY neurons in these processes. Whilst the Arc contains the largest proportion of *Lepr* neurons in the brain, it is important to note that this only comprises approximately 15% of total *Lepr* positive neurons [5,21–23]. It is plausible that not all *Lepr* neurons have the same effect and that the stimulation of such a specific subpopulation as we have done here will not show the same effect as that of systemic leptin administration. Interestingly, the effects are also contrary to that shown by the stimulation of all *Npy* neurons. Arc NPY has been shown to increase RQ, decrease energy expenditure, and decrease BAT thermogenesis. However, recent work from our group has shown that the specific deletion of *Npy* from *Agrp* neurons (approximately 80% of all *Npy* neurons) led to increased RQ and decreased energy expenditure suggesting that NPY in these *Npy*+/*Agrp*+ neurons may act to decrease RQ and increase energy expenditure [12]. This would be more consistent with the effects of *Npy*+/*Lepr*+ neurons that we have shown in this study.

Following the discovery of leptin, its secretion in proportion to body fat, and the hyperphagia and obesity present in leptin deficient mice and humans, there was considerable interest in the therapeutic potential of leptin for obese patients [24,25]. This was dampened by the further discovery that circulating levels of leptin are elevated in most obese patients compared to non-obese subjects and that they exist in a state of leptin resistance that in fact leads to the intake of extra calories and prevents sustained weight loss [26]. Leptin resistance has been shown to be a complex pathophysiological phenomenon with the underlying mechanisms still not entirely clarified. However, Arc NPY neurons have been shown to display leptin resistance under HFD fed conditions [27]. Our results here are consistent with these neurons no longer being able to drive metabolic effects, except for improving glucose tolerance, under chronically elevated leptin levels. Interestingly, we also show that whilst stimulation of *Npy*−/*Lepr*+ neurons in the Arc had little effect on metabolic parameters under normal or fasted conditions, they drove food intake and physical activity under HFD-fed conditions. Again, this is somewhat contrary to that expected as this population includes POMC neurons which should induce satiety and decrease feeding. However, it should be noted that here we targeted all *Npy*−/*Lepr*+ neurons and not POMC neurons specifically. Furthermore, whilst viral injection was targeted to the Arc, we saw expression with this Cre-on/Flp-off vector spread beyond the Arc to include the DMH, LHA, and PMV areas which are all known to express *Lepr* neurons with varying profiles and metabolic effects [19,21,28–31]. Further experiments and additional mouse models would be required to determine exactly which neurons are responsible for these effects. Nevertheless, together these data suggest that HFD feeding induces a breakdown in normal leptin signalling pathways and may explain why food intake is often exacerbated in overweight patients.

Previous studies have shown that hypothalamic NPY signalling has a strong inhibitory effect on bone formation, consistent with an energy conserving role for NPY whose levels are strongly upregulated during situations of negative energy balance [32]. In contrast, the central effects of leptin on bone are diverse, suggesting that differing populations of neurons are responsible for differing effects [33]. Here, our data are consistent with previous studies in demonstrating an interaction between leptin and NPY in the regulation of bone mass [10,34]. We now define that relationship to show that *Npy*+/*Lepr*+ neurons are capable of controlling bone mass independently of body weight. Furthermore, we show that while leptin signalling through non-*Npy* neurons can also increase bone mass through stimulating formation, this increase is proportional to increases in overall body weight. Thus, we have begun to define the differing neuronal populations responsible for the complex effects that central leptin signalling has on the skeleton.

Whilst the hypothalamus contains the greatest proportion of *Lepr* neurons, it also contains the greatest density of projections from *Lepr* neurons elsewhere in the brain [35]. Given the modest effects seen here with direct stimulation of *Npy*+/*Lepr*+ neurons compared to the critical role that NPY is believed to play in leptin's important functional effects, it is likely that leptin action on other local and/or distant *Lepr* neuronal populations results in projections acting on NPY neurons in the Arc to exert additional effects. Further studies will be required to determine whether these projections act on the same or differing subpopulations of NPY neurons as those expressing the *Lepr*. It is also important to note that a limitation of this study lies in the fact that we have used DREADD technology to activate and inhibit populations of *Lepr* neurons which may in fact respond differently to leptin. Whilst leptin may change the electrophysiological properties of some or all of these neurons, it may also alter metabolism via changes in transcriptional events without altering electrophysiological properties. It also remains unknown whether leptin actually employs the Gq/Gi pathway used in this paper to modulate neuronal activity.

AUTHOR CONTRIBUTIONS

NJL, HH Conceptualization, Funding acquisition, Project administration, and Supervision; NJL, JO Data curation; NJL, JO Formal analysis; NJL, YQ, JO, RFE Investigation; NJL, RT, HH Methodology; NJL, YQ Validation; NJL Writing — original draft; NJL, HH Writing — review & editing.

DATA AVAILABILITY

Data will be made available on request.

ACKNOWLEDGEMENTS

This work was funded by NHMRC Ideas grant 2001010 and Diabetes Australia grant Y21G-LEEN.

DECLARATION OF COMPETING INTEREST

The authors declare that they have no known competing financial interests or personal relationships that could have appeared to influence the work reported in this paper.

APPENDIX A. SUPPLEMENTARY DATA

Supplementary data to this article can be found online at https://doi.org/10.1016/j.molmet.2023.101790.

REFERENCES

[1] Casanueva FF, Dieguez C. Neuroendocrine regulation and actions of leptin. Front Neuroendocrinol 1999;20(4):317–63.
[2] Cohen P, Zhao C, Cai X, Montez JM, Rohani SC, Feinstein P, et al. Selective deletion of leptin receptor in neurons leads to obesity. J Clin Investig 2001;108(8):1113–21.
[3] de Luca C, Kowalski TJ, Zhang Y, Elmquist JK, Lee C, Kilimann MW, et al. Complete rescue of obesity, diabetes, and infertility in db/db mice by neuron-specific LEPR-B transgenes. J Clin Investig 2005;115(12):3484–93.
[4] Ducy P, Amling M, Takeda S, Priemel M, Schilling AF, Beil FT, et al. Leptin inhibits bone formation through a hypothalamic relay: a central control of bone mass. Cell 2000;100(2):197–207.
[5] Ring LE, Zeltser LM. Disruption of hypothalamic leptin signaling in mice leads to early-onset obesity, but physiological adaptations in mature animals stabilize adiposity levels. J Clin Investig 2010;120(8):2931–41.
[6] Biglari N, Gaziano I, Schumacher J, Radermacher J, Paeger L, Klemm P, et al. Functionally distinct POMC-expressing neuron subpopulations in hypothalamus revealed by intersectional targeting. Nat Neurosci 2021;24(7):913–29.
[7] Baskin DG, Breininger JF, Schwartz MW. Leptin receptor mRNA identifies a subpopulation of neuropeptide Y neurons activated by fasting in rat hypothalamus. Diabetes 1999;48(4):828–33.
[8] Luquet S, Perez FA, Hnasko TS, Palmiter RD. NPY/AgRP neurons are essential for feeding in adult mice but can be ablated in neonates. Science 2005;310(5748):683–5.
[9] Qi Y, Lee NJ, Ip CK, Enriquez R, Tasan R, Zhang L, et al. Agrp-negative arcuate NPY neurons drive feeding under positive energy balance via altering leptin responsiveness in POMC neurons. Cell Metab 2023;35(6):979–995 e977.
[10] Lee NJ, Qi Y, Enriquez RF, Clarke I, Ip CK, Wee N, et al. Energy partitioning between fat and bone mass is controlled via a hypothalamic leptin/NPY relay. Int J Obes 2020;44(10):2149–64.
[11] Kim JG, Sun BH, Dietrich MO, Koch M, Yao GQ, Diano S, et al. AgRP neurons regulate bone mass. Cell Rep 2015;13(1):8–14.
[12] Qi Y, Lee NJ, Ip CK, Enriquez R, Tasan R, Zhang L, et al. NPY derived from AGRP neurons controls feeding via Y1 and energy expenditure and food foraging behaviour via Y2 signalling. Mol Metab 2022;59:101455.
[13] Fenno LE, Mattis J, Ramakrishnan C, Hyun M, Lee SY, He M, et al. Targeting cells with single vectors using multiple-feature Boolean logic. Nat Methods 2014;11(7):763–72.
[14] Franklin KBJ, Paxinos G. The mouse brain in stereotaxic coordinates. San Diego: Academic Press; 1997.
[15] Lee NJ, Nguyen AD, Enriquez RF, Doyle KL, Sainsbury A, Baldock PA, et al. Osteoblast specific Y1 receptor deletion enhances bone mass. Bone 2011;48(3):461–7.
[16] Izquierdo AG, Crujeiras AB, Casanueva FF, Carreira MC. Leptin, obesity, and leptin resistance: where are we 25 years later? Nutrients 2019;11(11).
[17] Banks WA, DiPalma CR, Farrell CL. Impaired transport of leptin across the blood-brain barrier in obesity. Peptides 1999;20(11):1341–5.
[18] El-Haschimi K, Pierroz DD, Hileman SM, Bjorbaek C, Flier JS. Two defects contribute to hypothalamic leptin resistance in mice with diet-induced obesity. J Clin Investig 2000;105(12):1827–32.
[19] Rezai-Zadeh K, Yu S, Jiang Y, Laque A, Schwartzenburg C, Morrison CD, et al. Leptin receptor neurons in the dorsomedial hypothalamus are key regulators of energy expenditure and body weight, but not food intake. Mol Metab 2014;3(7):681–93.
[20] Paz-Filho G, Mastronardi C, Wong ML, Licinio J. Leptin therapy, insulin sensitivity, and glucose homeostasis. Indian J Endocrinol Metab 2012;16(Suppl. 3):S549–55.
[21] Flak JN, Myers Jr MG. Minireview: CNS mechanisms of leptin action. Mol Endocrinol 2016;30(1):3–12.
[22] Myers Jr MG, Munzberg H, Leinninger GM, Leshan RL. The geometry of leptin action in the brain: more complicated than a simple ARC. Cell Metab 2009;9(2):117–23.
[23] Scott MM, Lachey JL, Sternson SM, Lee CE, Elias CF, Friedman JM, et al. Leptin targets in the mouse brain. J Comp Neurol 2009;514(5):518–32.
[24] Farooqi IS, Yeo GS, Keogh JM, Aminian S, Jebb SA, Butler G, et al. Dominant and recessive inheritance of morbid obesity associated with melanocortin 4 receptor deficiency. J Clin Investig 2000;106(2):271–9.
[25] Zhang Y, Proenca R, Maffei M, Barone M, Leopold L, Friedman JM. Positional cloning of the mouse obese gene and its human homologue. Nature 1994;372(6505):425–32.
[26] Considine RV, Sinha MK, Heiman ML, Kriauciunas A, Stephens TW, Nyce MR, et al. Serum immunoreactive-leptin concentrations in normal-weight and obese humans. N Engl J Med 1996;334(5):292–5.
[27] Baver SB, Hope K, Guyot S, Bjorbaek C, Kaczorowski C, O'Connell KM. Leptin modulates the intrinsic excitability of AgRP/NPY neurons in the arcuate nucleus of the hypothalamus. J Neurosci 2014;34(16):5486–96.
[28] Donato Jr J, Silva RJ, Sita LV, Lee S, Lee C, Lacchini S, et al. The ventral premammillary nucleus links fasting-induced changes in leptin levels and coordinated luteinizing hormone secretion. J Neurosci 2009;29(16):5240–50.
[29] Faber CL, Deem JD, Phan BA, Doan TP, Ogimoto K, Mirzadeh Z, et al. Leptin receptor neurons in the dorsomedial hypothalamus regulate diurnal patterns of feeding, locomotion, and metabolism. Elife 2021;10.
[30] Leinninger GM, Jo YH, Leshan RL, Louis GW, Yang H, Barrera JG, et al. Leptin acts via leptin receptor-expressing lateral hypothalamic neurons to modulate the mesolimbic dopamine system and suppress feeding. Cell Metab 2009;10(2):89–98.
[31] Leinninger GM, Opland DM, Jo YH, Faouzi M, Christensen L, Cappellucci LA, et al. Leptin action via neurotensin neurons controls orexin, the mesolimbic dopamine system and energy balance. Cell Metab 2011;14(3):313–23.
[32] Baldock PA, Lee NJ, Driessler F, Lin S, Allison S, Stehrer B, et al. Neuropeptide Y knockout mice reveal a central role of NPY in the coordination of bone mass to body weight. PLoS One 2009;4(12):e8415.
[33] Reid IR, Baldock PA, Cornish J. Effects of leptin on the skeleton. Endocr Rev 2018;39(6):938–59.
[34] Wong IP, Nguyen AD, Khor EC, Enriquez RF, Eisman JA, Sainsbury A, et al. Neuropeptide Y is a critical modulator of leptin's regulation of cortical bone. J Bone Miner Res 2013;28(4):886–98.
[35] Patterson CM, Leshan RL, Jones JC, Myers Jr MG. Molecular mapping of mouse brain regions innervated by leptin receptor-expressing cells. Brain Res 2011;1378:18–28.

